Terr. Atmos. Ocean. Sci., Vol. 29, No. 6, 721-729, December 2018 doi: 10.3319/TAO.2018.08.24.01

NOTES AND CORRESPONDENCE

A note on the annual wobble excitation due to the seasonal atmospheric loading on continents

Sung-Ho Na[1, *], Jungho Cho[2], Ki-Weon Seo[3], Kook-Hyoun Youm[3], and Wenbin Shen[4]

[1] *KASI-SLR Observatory, Sejong, Korea*
[2] *Space Geodesy Group, Korea Astronomy and Space Science Institute, Daejeon, Korea*
[3] *Department of Earth Science Education, Seoul National University, Seoul, Korea*
[4] *Department of Geodesy and Geomatics, Wuhan University, Wuhan, China*

Article history:
Received 23 February 2018
Revised 5 July 2018
Accepted 24 August 2018

Keywords:
Polar motion, Atmospheric excitation, Siberia

Citation:
Na, S.-H., J. Cho, K.-W. Seo, K.-H. Youm, and W. Shen, 2018: A note on the annual wobble excitation due to the seasonal atmospheric loading on continents. Terr. Atmos. Ocean. Sci., 29, 721-729, doi: 10.3319/TAO.2018.08.24.01

ABSTRACT

Northern Eurasian continent has been regarded to contribute as the major source area, of which seasonal atmospheric pressure loading and unloading cycle leads to the annual wobble of the Earth. In the early days when reliable data of global coverage were not accessible, this dominance has remained as only a hypothesis. Nowadays, however, European Centre for Medium-Range Weather Forecasts and National Centers for Environmental Prediction produce reliable datasets, therefore, such unique feature has become clearer with quantitative evidences. Having both the Earth's polar motion and the global atmospheric state known with unprecedented accuracy, we hereby identify and scrutinize whether Siberia and Manchuria dominate the annual polar motion of the Earth.

1. INTRODUCTION

Although the Earth rotation is fairly uniform and consistent in times of days or thousand years, at close observation aided by space geodetic measurements, the Earth's spin rotation axis undergoes wobbling which is rather small (usually its amplitude is a few meters on the Earth's surface) but quite complicated in nature. Change in Earth rotation can be categorized into two kinds; (1) change in its angular spin rate or length of day (LOD) and (2) change in the orientation of the Earth's spin axis, that is, precession-nutation and wobble. LOD variation associated with the seasonal change in the global atmospheric wind pattern had been suspected and was discovered in the middle of the last century. Other interesting topics are involved with secular and decadal variations of LOD. Precession and nutation are forced motions of the Earth's rotational axis in the celestial sphere due mainly to lunisolar tidal force on the equatorial bulge of the Earth, and therefore, they are not associated with the processes in the Earth. In modern and formal definition, wobble is the movement of the Earth's rotational pole in the terrestrial reference system of which frequency is either greater than -0.5 or smaller than -1.5 cycle per sidereal day [IERS Conventions 2010 (Petit and Luzum 2010); here the minus sign refers to 'retrograde', i.e., the reverse of the Earth's spin]. In Fig. 1, recent polar motion since 1981 is illustrated based on the dataset of IERS EOP C04. EOP C04 is basically daily basis dataset composed of pole position coordinates and their uncertainties with changes in LOD and UT1, and it is a combined solution from different space geodetic observations; VLBI, GPS, SLR, and DORIS (Bizouard and Gambis 2009). Annual wobble is one of the two main components of Earth's wobbling motion. While Chandler wobble excitation mechanism has been controversial for a long time, it is evident that annual wobble is driven by geophysical phenomena having periodic

* *Corresponding author*
E-mail: sunghona@ust.ac.kr

seasonal variations (see for example, Munk and MacDonald 1960; Lambeck 1980; Gross 2009). And it has been presumed since early times that Siberia does a noticeable role in the annual wobble excitation, i.e., periodic loading/unloading of air mass over the wide Siberian land may result in major contribution on the Earth's annual wobble (Munk and MacDonald 1960). Although the torque associated with the seasonal changes in the global atmospheric circulation pattern result in the excitation of the same order of magnitude, however, such contribution on each continents are generally regarded as smaller than that induced by mass changes.

Information of worldwide weather are gathered and assimilated in European Centre for Medium-Range Weather Forecasts (ECMWF) and National Centers for Environmental Prediction (NCEP) for the purpose of weather forecasting as well as to provide datasets necessary for scientific investigations. The 6-hr period global data coverage by ECMWF on wind velocity and barometric pressure can be used to infer the atmospheric excitation of Earth rotation. Monthly average values of surface atmospheric pressure in the year of 2016 are illustrated in Fig. 2. The pressure values in this figure were not adjusted down to sea-level but taken as on-site raw values so that they are used for evaluation of excitation integral. However pressure deviation from local average value should be used unto the integral unless whole globe is simultaneously considered. Monthly average values of differential surface atmospheric pressure from local yearly average in the year of 2016 are illustrated in Fig. 3. On the northern part of Eurasian continent, i.e., Siberia and Manchuria, high atmospheric pressure exists from October to March, while low atmospheric pressure prevails from May to August. For closer comparison between winter and summer seasons January and July average pressure as well as the deviatoric pressure from the local year average are illustrated together in Fig. 4. Although this seasonal loading/unloading cycle has been thought as the main input to annual wobble since the beginning of last century (Munk and MacDonald 1960), reliable estimations have been deferred until the advent of accurate source of information, such as ECMWF dataset or comparable sort.

In this study, we compare (1) the observed geodetic excitation inferred from the recent polar motion data and (2) the calculated atmospheric excitation due to seasonal atmospheric loading/unloading on Northern Eurasia as well as four other continents, namely, North America, South America, Australia, and Africa. We used IERS EOP C04 and ECMWF atmospheric pressure datasets each.

2. METHODOLOGY

For complex polar motion $p_c(t) = x_p(t) - iy_p(t)$ and complex excitation function $\chi_c(t) = \chi_1(t) + i\chi_2(t)$, one can define their Fourier transform pairs as $P(\omega)$ and $X(\omega)$. Then a simple relation holds between $P(\omega)$ and $X(\omega)$ in the frequency domain as follows (Na 2013).

$$\Omega X(\omega) = (\Omega - \omega) P(\omega) \tag{1}$$

In Eq. (1), Ω is the Chandler frequency; $\Omega = \frac{\omega_0}{433.5}\left(1 + \frac{i}{2Q}\right)$ with the Earth's rotation angular velocity ω_0 and the Chandler wobble quality factor Q (taken as 100). Therefore, from a dataset of polar motion, one can derive its excitation function by Fourier transform and successive manipulation according to Eq. (1) and then inverse Fourier transform. Usually the excitation function derived from polar motion time series through this procedure is called 'geodetic excitation'.

With known perturbation due to certain geophysical

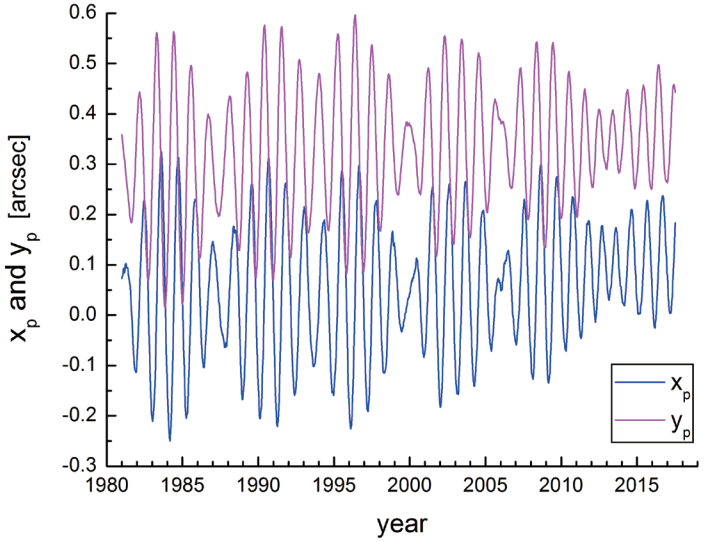

Fig. 1. Two components x_p and y_p of polar motion since 1981 (IERS EOP C04).

Fig. 2. Monthly average barometric pressure distribution on the globe in 2016 (ECMWF). Sea level reduction not applied. These values are to be used directly for the excitation integral.

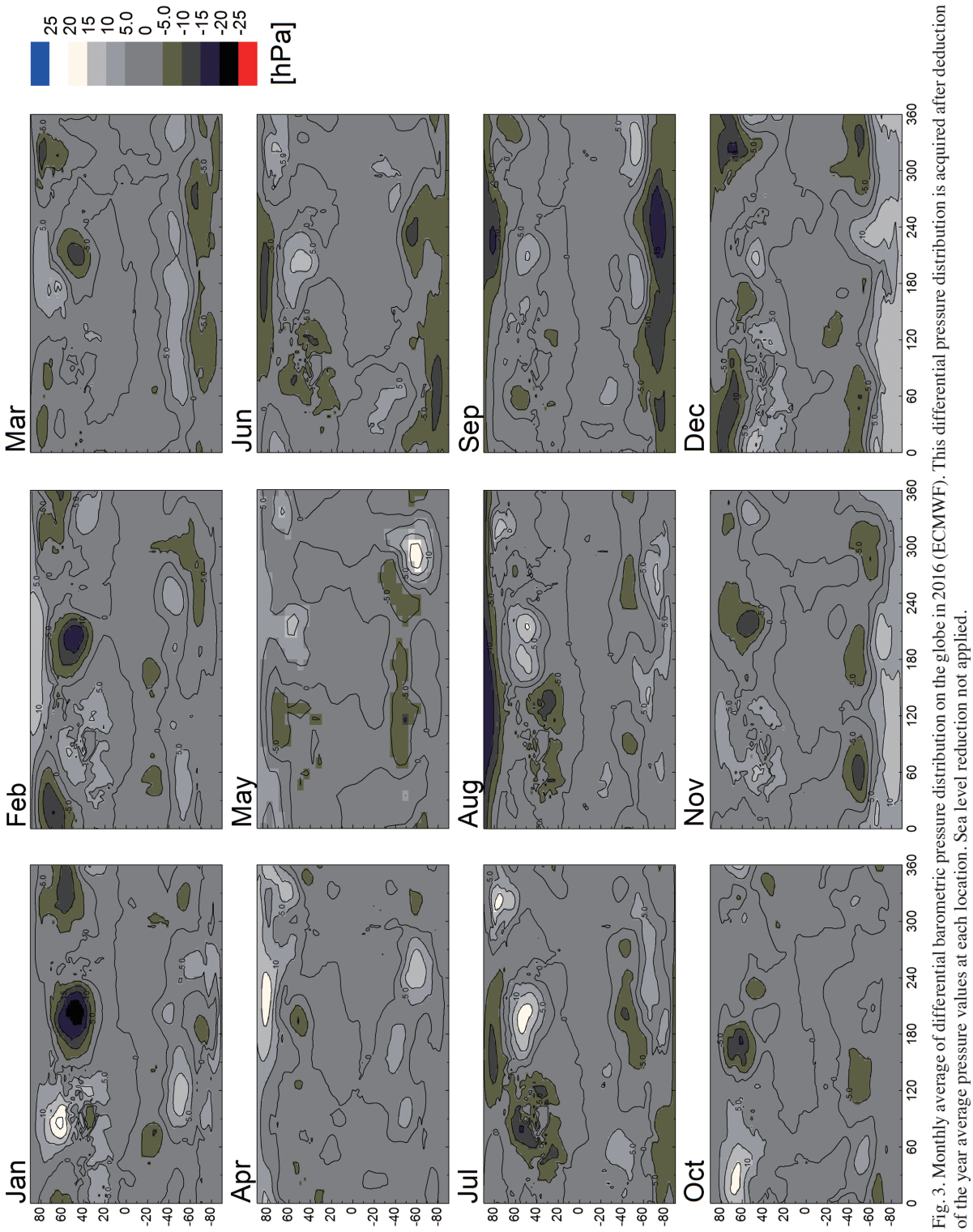

Fig. 3. Monthly average of differential barometric pressure distribution on the globe in 2016 (ECMWF). This differential pressure distribution is acquired after deduction of the year average pressure values at each location. Sea level reduction not applied.

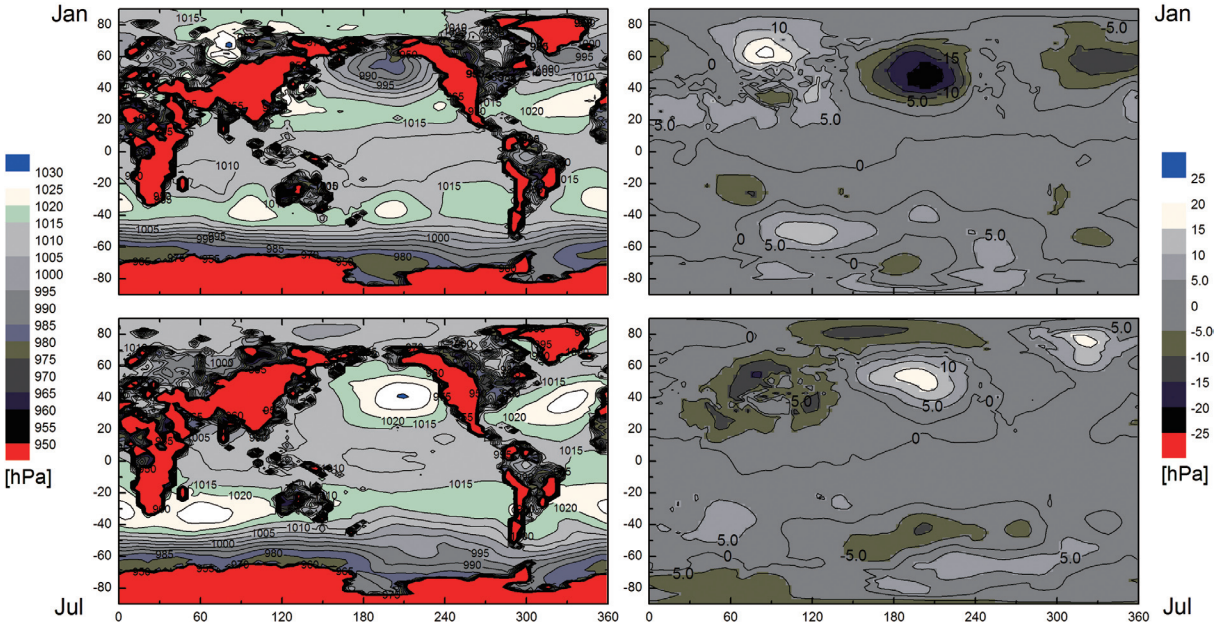

Fig. 4. January and July average barometric pressure distributions on the globe in 2016 (ECMWF) and their differential values after deduction of the year average pressure. Sea level reduction not applied.

processes on the Earth's surface or its interior, polar motion excitation function can be expressed again as follows (Gross 2009).

$$\chi_i = \frac{1.608 h_i}{(C - A)\omega_0} + \frac{1.100 \Delta I_{i3}}{C - A} \quad (i = 1, 2) \tag{2}$$

where C and A are the two principal moments of inertia of the Earth along z-axis and x-axis, and h_i and ΔI_{i3} are the imposed perturbing angular momentum and the perturbation in the Earth's inertia tensor. In case of considering barometric pressure loading/unloading only, the polar motion excitation function can be expressed as follows (Eubanks 1993; Gross 2009).

$$\chi_1 = -\frac{1.100 a^4}{(C - A) g} \int_0^{2\pi} \int_0^{\pi} \Delta P(\theta, \lambda) \cos\theta \sin^2\theta \cos\lambda \, d\theta d\lambda \tag{3a}$$

$$\chi_2 = -\frac{1.100 a^4}{(C - A) g} \int_0^{2\pi} \int_0^{\pi} \Delta P(\theta, \lambda) \cos\theta \sin^2\theta \sin\lambda \, d\theta d\lambda \tag{3b}$$

where ΔP is the excessive barometric pressure, and a and g are the radius and surface gravity of the Earth.

To extract seasonal variation (1-year period sinusoidal oscillation) from given time series of polar motion, we used least square fitting based on the following model (Chung and Na 2016).

$$x_p(t) = x_p(t_0) + L_x(t - t_0) + \sum_{k=1}^{2} A_k \cos[\Omega_k (t - t_0) + \phi_k^x] \tag{4a}$$

$$y_p(t) = y_p(t_0) + L_y(t - t_0) - \sum_{k=1}^{2} B_k \sin[\Omega_k (t - t_0) + \phi_k^y] \tag{4b}$$

where Ω_1 and Ω_2 are the frequencies of Chandler and annual wobbles. A_k and B_k are the amplitudes of each components. Similarly, least square error fittings have been done on the observed or calculated excitation functions as follows.

$$\chi_1(t) = \chi_1(t_0) + L_1(t - t_0) + \sum_{k=1}^{2} C_k \cos[\Omega_k (t - t_0) + \phi_k^1] \tag{5a}$$

$$\chi_2(t) = \chi_2(t_0) + L_2(t - t_0) + \sum_{k=1}^{2} D_k \sin[\Omega_k (t - t_0) + \phi_k^2] \tag{5b}$$

3. RESULTS

The geodetic (observed) excitation function was acquired from the polar motion dataset, IERS EOP C04. The χ_1 component of the observed excitation function after 2010 is illustrated in Fig. 5. Its five graphs are (1) geodetic excitation acquired from polar motion data, (2) atmospheric excitation (wind + pressure: global), (3) atmospheric excitation (wind only: global), (4) atmospheric excitation (pressure only: global), and (5) atmospheric excitation (pressure: Siberia and Manchria). Similarly the excitation function χ_2 after 2010 is illustrated in Fig. 6. It can be found that atmospheric pressure excitation on χ_2 is roughly about half of the observed excitation.

Figure 7 shows the geodetic excitation function and together with its annual oscillation component acquired by least square fitting. It is noted that fitting itself was done on seventeen-year dataset, while only the latter five-year data

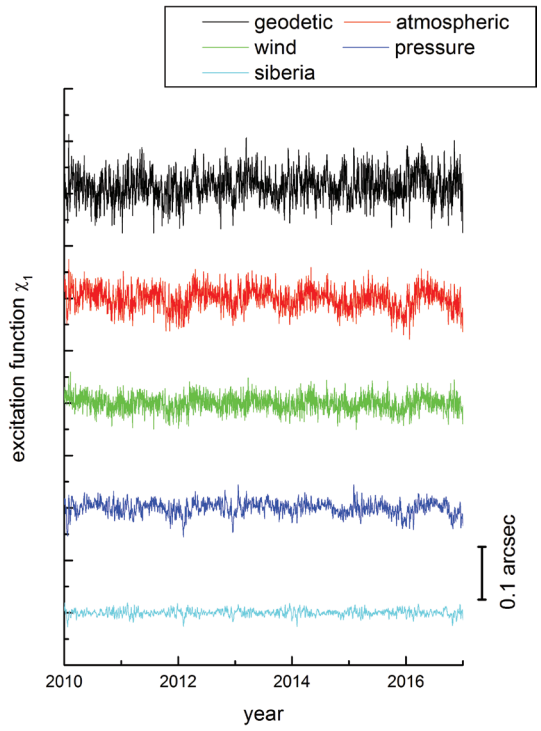

Fig. 5. Comparison of polar motion excitation function χ_1. From top to bottom, they are geodetic excitation, atmospheric excitation (wind and pressure), atmospheric excitation (wind only), atmospheric excitation (pressure only), and atmospheric excitation (pressure of Siberia and Manchuria).

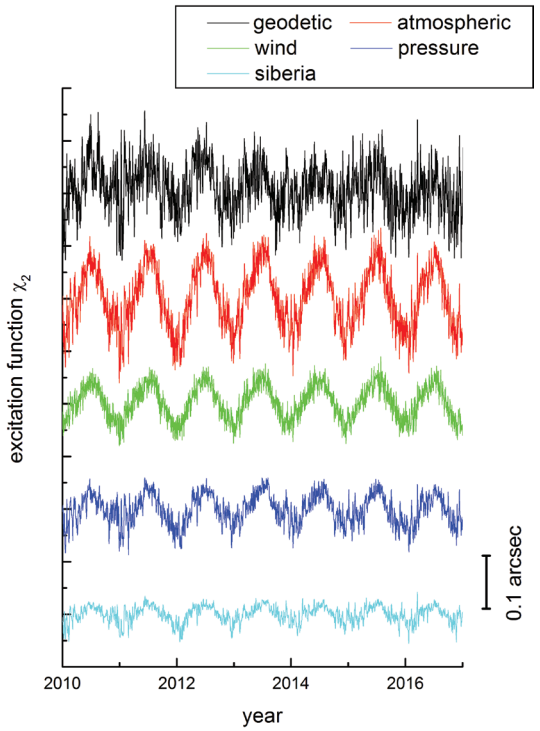

Fig. 6. Comparison of polar motion excitation function χ_2. From top to bottom, they are geodetic excitation, atmospheric excitation (wind and pressure), atmospheric excitation (wind only), atmospheric excitation (pressure only), and atmospheric excitation (pressure of Siberia and Manchuria).

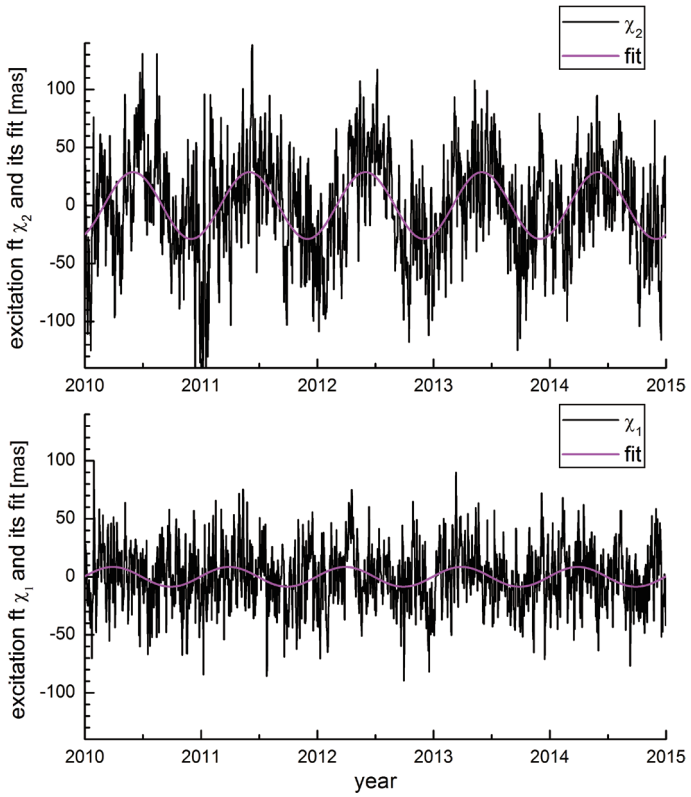

Fig. 7. Five-year (2010 - 2015) geodetic excitation function and its annual oscillation fitting. The fitting itself has been done on the 17 years long dataset.

and fit are shown on the figure. Although not shown here, the annual wobble component is acquired similarly on the polar motion. Figure 8 shows two elliptical loci of (1) the annual wobble component and (2) the annual excitation.

We repeated the computation for atmospheric pressure excitation on other continents, North America, South America, Australia, and Africa. The amplitudes of the geodetic excitation and calculated excitation due to atmospheric pressure on the five continents are provided in Table 1. And, in different forms, the total-observed and calculated excitations are again illustrated together in Fig. 9 for their comparison. It has been found that the atmospheric pressure loading/unloading annual cycle on Siberia and Manchuria gave rise to 15.61 milliarcsec excitation in χ_2 component, which is 54% of total excitation observed, while the same area gave rise to much smaller χ_1 excitation. The atmospheric loading/unloading on Australia gave rise to rather large excitation both on χ_1 and χ_2.

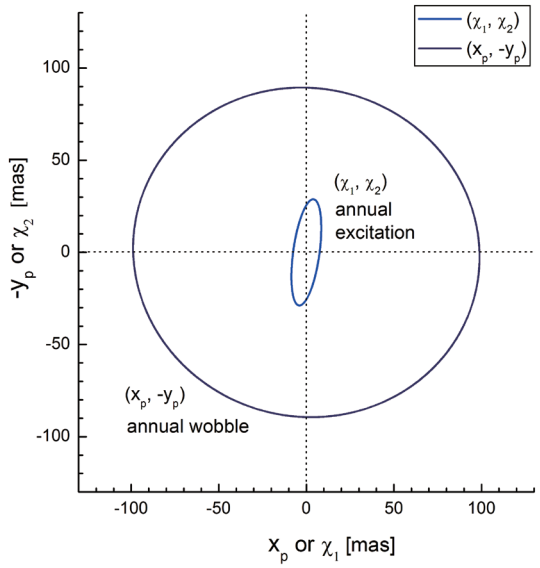

Fig. 8. Two dimensional drawing of annual polar motion and annual excitation. Both are least square fit graphs of same scale. The direction of y_p axis is reverse of χ_2.

4. DISCUSSION AND CONCLUSION

Atmospheric seasonal loading/unloading cycle on Siberia and Manchuria results in more than fifty percentage (54%) of the observed excitation. And this holds not only for χ_2 but also for total amplitude including χ_1 component. To see more clearly the seasonal atmospheric loading cycle on Siberia, which is shown in the monthly average barometric pressure distribution in Figs. 2 and 3, another kinds of maps are drawn as Figs. 10 and 11, which show the January and July monthly average barometric pressure on the northern hemisphere using equal area projection. From the maps of Figs. 10 and 11, one can readily see the atmospheric loading cycle on the northern Eurasia - Siberia and Manchuria. Also one can see why χ_1 excitation associated with Siberia and Manchuria area is much smaller than χ_2 excitation because the center of the area (Siberia + Manchuria) is quite close to y-axis (longitude $\lambda = +90^\circ$).

It should be noted that high/low barometric pressure on the vast area of oceans has almost no contribution to polar motion excitation. This is due to the fact that ocean water would re-distribute under atmospheric pressure (often called 'inverted barometer') so that ocean bottom pressure exerts virtually no seasonal perturbation on the Earth's rotation.

Although the amplitude of χ_2 component of the observed excitation is much larger than that of χ_1, the annual polar motion has been more or less circular (Fig. 8). Other feature is that high frequency components exist in large amounts in both χ_1 and χ_2 components of the observed excitation (Figs. 5, 6, and 7), in other words, the polar motion time series show much smoother variation than its excitation time series. Actually, this smaller amount of high frequency content is due the fact that polar motion is, in a sense, a time integral of the polar motion excitation function.

Atmospheric pressure excitation functions calculated

Table 1. Observed total geodetic excitation and five calculated excitation function pairs defined as Eqs. (5a) - (5b). Calculated ones are due to the atmospheric loading/unloading on each different continents. All the amplitudes and phases were determined by least square fittings.

	χ_1 [mas]	ϕ^1_{ann} [rad]	χ_2 [mas]	ϕ^2_{ann} [rad]
geodetic ex. (total)	8.53	4.77	28.80	5.25
cal. ex. (Siberia)	0.32	1.89	15.61	0.14
cal. ex. (N. Amer.)	0.93	4.92	0.58	3.08
cal. ex. (S. Amer.)	1.75	4.74	2.82	3.17
cal. ex. (Australia)	3.42	1.58	3.48	0.00
cal. ex. (Africa)	6.56	4.84	1.92	0.08

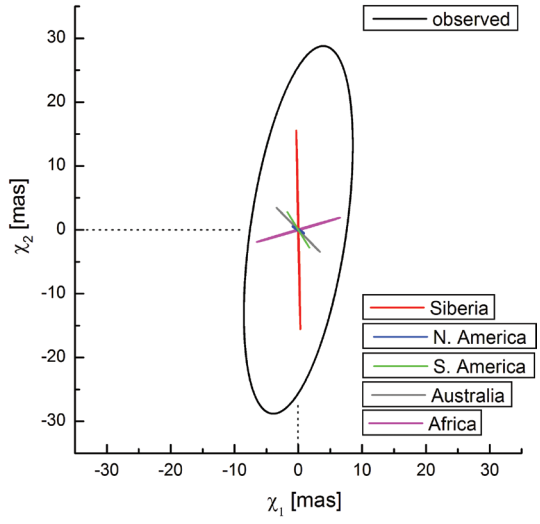

Fig. 9. Comparison of geodetic excitation and five annual excitation fits on the atmospheric pressure loading/unloading on the 5 continents – Eurasia, N. America, S. America, Australia, and Africa.

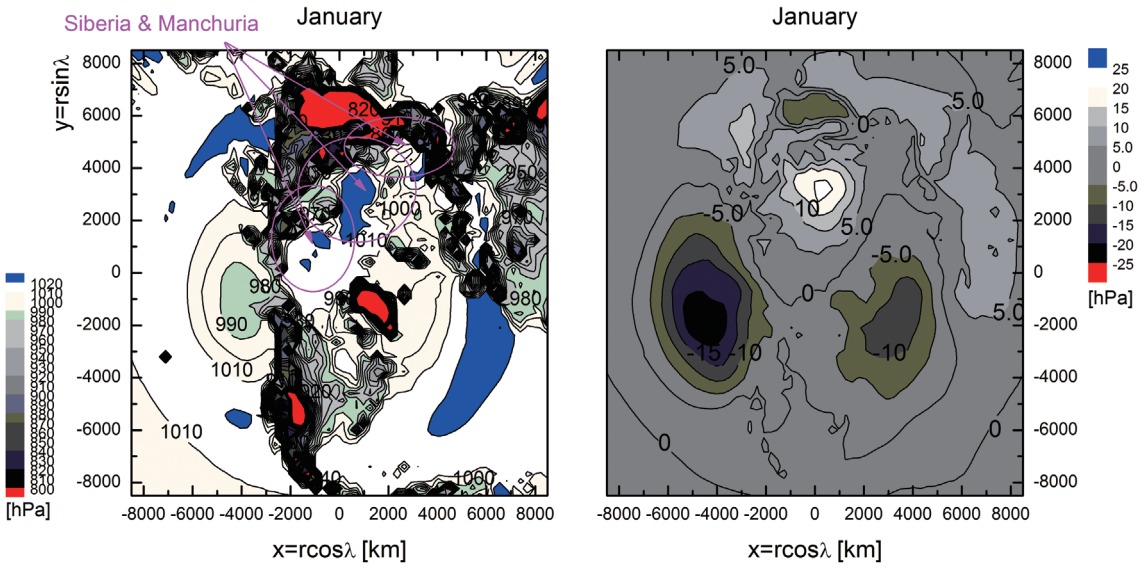

Fig. 10. January average of atmospheric pressure on the northern hemisphere (left panel) and corresponding differential pressure distribution after deduction of the year average value (right panel). In left panel, areas marked pink are northern parts of the Eurasian continent, which correspond to Siberia and Manchuria and under high barometric pressure.

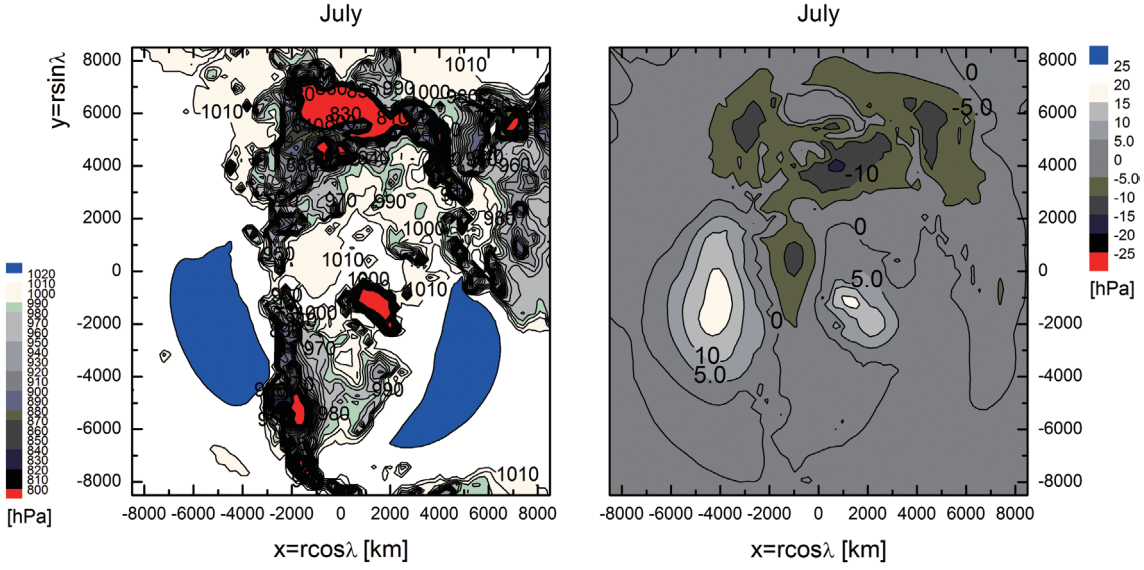

Fig. 11. July average of atmospheric pressure on the northern hemisphere (left panel) and corresponding differential pressure distribution after deduction of the year average value (right panel). In left panel, Siberia and Manchuria are under comparatively low barometric pressure.

using ECMWF data on other continents, North America, South America, and Australia in the given time span (2010 - 2015) have been smaller than that of Siberia and Manchuria. However Australia, having comparatively smaller area, has contributed larger portion of excitation than other continents, particularly in χ_1 component. This is due to its location [central longitude $\lambda = +135^\circ$ and colatitude $\theta = 115^\circ$, see Eqs. (3a) - (3b)] so that seasonal loading cycle successfully exerts same large amplitude both in χ_1 and χ_2. It is also notable that North American continent has a small fraction of contribution to the polar motion excitation. Africa, being centered near the equator, may be overlooked as to exert small amount of loading excitation. However, it does affect in considerable amount as shown in Fig. 9 and Table 1.

Total atmospheric excitation χ_2 acquired from ECMWF data exceeds the observed excitation during the whole time span as observed in Fig. 6. Had we have data for other possible causes, such as, ground water level change or

glacier melting rate variation, that inequality might be reasonably explained.

From the comparison of observed geodetic excitation inferred from IERS C04 polar motion dataset and calculated excitation function via integration of ECMWF pressure data, we hereby confirm that the atmospheric seasonal loading cycle in the area of Siberia and Manchuria with their neighbors in the Northern Eurasian continent, plays the major role in the annual wobble of the Earth's spin rotation axis in the Earth's reference system.

Acknowledgements This study has been supported from Korea Astronomy and Space Science Institute as one of its space geodesy subprojects. Sung-Ho Na wishes to turn his gratitudes to the Lord Jesus Christ.

REFERENCES

Bizouard, C. and D. Gambis, 2009: The Combined Solution C04 for Earth Orientation Parameters Consistent with International Terrestrial Reference Frame 2005. In: Drewes, H. (Ed.), Geodetic Reference Frames, International Association of Geodesy Symposia, Vol. 134, Springer, Berlin, Heidelberg, 265-270, doi: 10.1007/978-3-642-00860-3_41. [Link]

Chung, T. W. and S. H. Na, 2016: A Least Square Fit Analysis on the Earth's Polar Motion Time Series: Implication against Smylie's Conjecture. *Geophysics and Geophysical Exploration*, **19**, 91-96, doi: 10.7582/GGE.2016.19.2.091. [Link]

Eubanks, T. M., 1993: Variations in the orientation of the Earth. In: Smith, D. E. and D. L. Turcotte (Eds.), Contributions of Space Geodesy to Geodynamics: Earth Dynamics, Vol. 24, American Geophysical Union, doi: 10.1029/GD024p0001. [Link]

Gross, R. S., 2009: Earth Rotation Variations – Long Period. In: Herring, T. A. (Ed.), Physical Geodesy, Treatise on Geophysics, Vol. 11, Elsevier, Amsterdam, 239-294.

Lambeck, K., 1980: The Earth's Variable Rotation: Geophysical Causes and Consequences, Cambridge University Press, 460 pp.

Munk, W. H. and G. J. F. MacDonald, 1960: The Rotation of the Earth: A Geophysical Discussion, Cambridge University Press, 323 pp.

Na, S. H., 2013: Earth Rotation – Basic Theory and Features. In: Jin, S. (Ed.), Geodetic Sciences: Observations, Modeling and Applications, Intech, 285-327, doi: 10.5772/54584. [Link]

Petit, G. and B. Luzum, 2010: International Earth Rotation and Reference Systems Service Technical Note 36, IERS Conventions Centre, Verlag des Bundesamts für Kartographie und Geodäsie Frankfurt am Main.